Author Contributions:

Conceptualization: Daniel J. Ford, Gavin H. Tilstone, Jamie D. Shutler, Vassilis Kitidis, Katy L. Sheen, Giorgio Dall'Olmo
Data curation: Daniel J. Ford, Iole B. M. Orselli
Formal analysis: Daniel J. Ford
Funding acquisition: Gavin H. Tilstone, Jamie D. Shutler, Vassilis Kitidis
Investigation: Daniel J. Ford, Iole B. M. Orselli
Methodology: Daniel J. Ford, Gavin H. Tilstone, Jamie D. Shutler, Vassilis Kitidis, Katy L. Sheen

Mesoscale Eddies Enhance the Air-Sea CO₂ Sink in the South Atlantic Ocean

Daniel J. Ford[1,2,3] [iD], Gavin H. Tilstone[1] [iD], Jamie D. Shutler[2] [iD], Vassilis Kitidis[1] [iD], Katy L. Sheen[2], Giorgio Dall'Olmo[1,4] [iD], and Iole B. M. Orselli[5] [iD]

[1]Plymouth Marine Laboratory, Plymouth, UK, [2]College of Life and Environmental Sciences, University of Exeter, Penryn, UK, [3]Now at Faculty of Environment, Science and Economy, University of Exeter, Penryn, UK, [4]Now at Istituto Nazionale di Oceanografia e di Geofisica Sperimentale, Trieste, Italy, [5]Laboratório de Estudos dos Oceanos e Clima, Instituto de Oceanografia, Universidade Federal do Rio Grande (FURG), Rio Grande, Brazil

Abstract Mesoscale eddies are abundant in the global oceans and known to affect oceanic and atmospheric conditions. Understanding their cumulative impact on the air-sea carbon dioxide (CO_2) flux may have significant implications for the ocean carbon sink. Observations and Lagrangian tracking were used to estimate the air-sea CO_2 flux of 67 long lived (>1 year) mesoscale eddies in the South Atlantic Ocean over a 16 year period. Both anticyclonic eddies originating from the Agulhas retroflection and cyclonic eddies originating from the Benguela upwelling act as net CO_2 sinks over their lifetimes. Anticyclonic eddies displayed an exponential decrease in the net CO_2 sink, whereas cyclonic eddies showed a linear increase. Combined, these eddies significantly enhanced the CO_2 sink into the South Atlantic Ocean by $0.08 \pm 0.04\%$. The studied eddies constitute a fraction of global eddies, and eddy activity is increasing; therefore, explicitly resolving eddies appears critical when assessing the ocean carbon sink.

Plain Language Summary Ocean mesoscale eddies can form when part of a main current becomes separated or through internal ocean instabilities which form circular rotating currents that propagate across the oceans. These eddies last from weeks to years and can modify the ocean properties of the water captured within them, which in turn affects the net exchange of carbon between this water and the atmosphere. Little is known about how these eddies modify the absorption of carbon across the global ocean, collectively referred to as the ocean carbon sink, despite them being ubiquitous features of the global oceans. Using in situ and satellite-based observations, we show that eddies in the South Atlantic Ocean enhance the absorption of carbon from the atmosphere, thus modifying the ocean to be a stronger net sink of carbon. These results are important as they quantify how much eddies contribute to the absorption of carbon from the atmosphere to the ocean, and highlight the need to include eddies when assessing ocean carbon budgets.

1. Introduction

Mesoscale eddies, characterized by radii on the order of 100 kilometers (km) and lifetimes of weeks to years, are ubiquitous in the global oceans (Chelton et al., 2011; Pegliasco et al., 2022). Eddies modify the physical (Laxenaire et al., 2019; Nencioli et al., 2018), biological (Carvalho et al., 2019; Dufois et al., 2016; Lehahn et al., 2011; Roughan et al., 2017), and chemical (Arhan et al., 2011; Chen et al., 2007; Orselli, Goyet, et al., 2019; Orselli, Kerr, et al., 2019) characteristics of the ocean compared to the surrounding waters and can be advected far away from their origin. Alteration of the ocean surface conditions can modulate the air-sea exchange of CO_2 through changes in the partial pressure of CO_2 ($pCO_{2(sw)}$) (Chen et al., 2007; Jones et al., 2017; Orselli, Kerr, et al., 2019; Song et al., 2016), solubility of CO_2, and the overlying atmospheric conditions (Frenger et al., 2013; Pezzi et al., 2021; Souza et al., 2021). Despite their abundance, few studies have investigated the role of eddies in the air-sea exchange of CO_2 (Chen et al., 2007; Jones et al., 2017; Pezzi et al., 2021) and estimated their cumulative impact on the oceanic CO_2 sink (Orselli, Kerr, et al., 2019).

Anticyclonic eddies generally display high-pressure centers, displace isopycnals downwards inducing downwelling, and have higher sea surface temperatures (SST) than the surrounding environment (McGillicuddy, 2016). The CO_2 solubility in seawater decreases with increasing temperature (Weiss, 1974), and biological activity would hypothetically decrease due to lower nutrient inputs into the surface layer caused by downwelling (Angel-Benavidez et al., 2016; Gaube et al., 2014; Liu et al., 2018). Therefore, these anticyclonic features could

Geophysical Research Letters

increase $pCO_{2(sw)}$ and act as weak CO_2 sinks or even sources of CO_2 to the atmosphere. Cyclonic eddies follow the opposite convention with low-pressure centers, lower SST (Chen et al., 2007), elevated isopycnals inducing upwelling, enhanced biological activity due to upwelled nutrients (Angel-Benavidez et al., 2016) and therefore potentially decreasing $pCO_{2(sw)}$, and enhancing the CO_2 sink.

Mesoscale eddies are, however, intricate structures, and the way they modify the air-sea CO_2 fluxes is more complex. Jones et al. (2017) identified that both anticyclonic and cyclonic eddies were hotspots for CO_2 drawdown in the Southern Ocean. Orselli, Kerr, et al. (2019) showed that anticyclonic (Agulhas) eddies are a stronger CO_2 sink than the surrounding water in the South Atlantic. By contrast, Pezzi et al. (2021) identified an anticyclonic eddy as a CO_2 source and Chen et al. (2007) reported that a single cyclonic eddy in the North Pacific weakened the CO_2 sink by ~17%. Song et al. (2016) showed that the way in which eddies modify the air-sea CO_2 flux can change seasonally in the Southern Ocean: anticyclonic eddies were stronger CO_2 sources in winter and stronger CO_2 sinks in summer, and the opposite was found for cyclonic eddies. The ability of mesoscale eddies to modify the CO_2 flux as they age (Orselli, Kerr, et al., 2019), may also vary seasonally.

The South Atlantic Ocean contributes ~10% to the global ocean CO_2 sink (e.g., Landschützer et al., 2014). The basin has some of the largest long-lived (>1 year) anticyclonic eddies globally, originating from the Agulhas retroflection (Lutjeharms, 2006), and can propagate to the Brazilian Coast (Guerra et al., 2018). In conjunction, cyclonic eddies from the Benguela upwelling system propagate across the basin (Chelton et al., 2011; Pegliasco et al., 2022; Rubio et al., 2009). The effect of eddies on the air-sea CO_2 flux, differences between anticyclonic and cyclonic, and their role in the global ocean CO_2 sink requires further investigation, especially since eddy kinetic energy has been increasing globally (Martínez-Moreno et al., 2021).

The objective of this study is to estimate the air-sea CO_2 flux of long-lived mesoscale eddies in the South Atlantic Ocean using satellite and in situ observations. A total of 67 eddies, 36 Agulhas anticyclonic and 31 Benguela cyclonic, were tracked using satellite observations (2002–2018) and Lagrangian cumulative air-sea CO_2 fluxes were estimated in order to assess their role in the South Atlantic CO_2 sink. To help understand which processes are controlling the change in flux over the lifetime of each eddy, the $pCO_{2(sw)}$ timeseries for each eddy was decomposed into the thermal and non-thermal drivers.

2. Data and Methods

2.1. Sea Surface Temperature, Salinity, Biological and Wind Speed Data

Daily 4 km chlorophyll a (chl a) composites were calculated from Moderate Resolution Imaging Spectroradiometer on Aqua (MODIS-A) Level 1 granules, downloaded from the National Aeronautics Space Administration (NASA) Ocean Color website (https://oceancolor.gsfc.nasa.gov/; accessed 10 December 2020), using SeaDAS v7.5, and applying the standard OC3-CI algorithm for chl a (https://oceancolor.gsfc.nasa.gov/atbd/chlor_a/; accessed 15 December 2020). Coincident 4 km daily composites of SST (NASA OBPG, 2015) and photosynthetically active radiation (PAR) (NASA OBPG, 2017b) were also downloaded from the NASA ocean color website (https://oceancolor.gsfc.nasa.gov/; accessed 10 December 2020). SST, PAR and chl a were used to estimate net primary production (NPP) using the Wavelength Resolving Model (Morel, 1991) with the look up table described in Smyth et al. (2005). Daily net community production (NCP) composites were generated using NPP and SST data with the algorithm NCP-D described in Tilstone et al. (2015). The chl a, NPP, NCP and SST satellite algorithms were shown to perform best in the South Atlantic with respect to in situ data and accounting for uncertainties in both in situ and satellite data (Ford et al., 2021). Daily 8 km sea surface salinity (SSS) composites were retrieved from the Copernicus Marine Service (CMEMS) physics reanalysis product (GLORYSV12) (CMEMS, 2021). Daily 0.25° resolution wind speed at 10 m were downloaded from Remote Sensing Systems Cross-Calibrated Multi-Platform (CCMP) product (Wentz et al., 2015). All data were retrieved for the period July 2002 to December 2018.

2.2. AVISO+ Mesoscale Eddy Tracking Product and Lagrangian Tracking

The satellite altimetry AVISO+ Mesoscale Eddy Product META3.1exp (Mason et al., 2014; Pegliasco et al., 2021, 2022) was used to identify the trajectories of mesoscale eddies within the South Atlantic Ocean, and provides daily estimates of the eddy location and radius. Anticyclonic (Agulhas) eddies were analyzed if: (a)
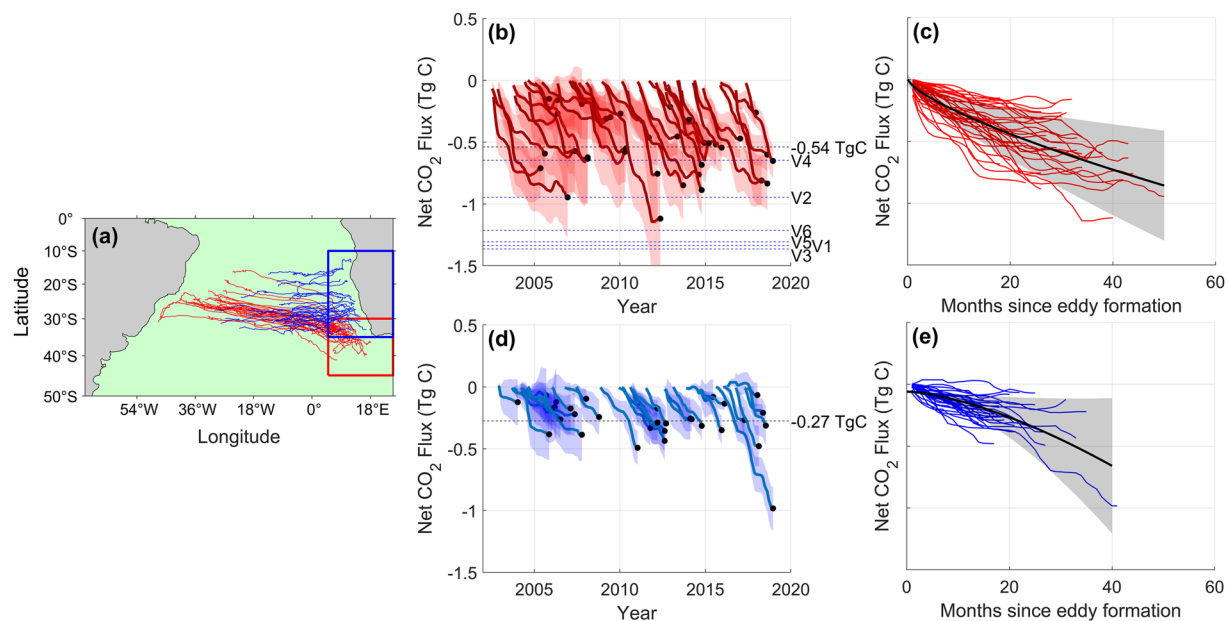
Figure 1. (a) Trajectories of the 36 anticyclonic (red lines) and 31 cyclonic (blue lines) eddies. Red and blue boxes indicate the formation region for the anticyclonic and cyclonic eddies respectively. (b) Red lines indicate the cumulative net CO_2 flux for the 36 anticyclonic eddies, where shading is the propagated uncertainty. Black dots indicate the cumulative net CO_2 flux at eddy dissipation. Black dashed line indicates the median cumulative net CO_2 flux at eddy dissipation (i.e., median of black dots). Blue dashed lines indicate the estimates for 6 anticyclonic eddies presented in Orselli, Kerr, et al. (2019). (c) Cumulative net CO_2 flux for the 36 anticyclonic eddies plotted since eddy formation. Black line indicates a power law fit ($y = a * x^b + c$) for the temporal evolution of the net CO_2 flux of the 36 anticyclonic eddies, where shading indicates the 95% confidence limits. (d) The same as (b), and (e) the same as (c) but for the 31 cyclonic eddies.

the eddy trajectory started in the Agulhas retroflection region (30°S–40°S; 5°E–25°E; Figure 1a); (b) the eddy trajectory was longer than 1 year; and (c) the trajectory crossed 0°E into the South Atlantic gyre region. These criteria identified 36 anticyclonic eddies for analysis between July 2002 and December 2018, that entered the South Atlantic as a single trajectory from formation to dissipation, with limited interactions with other eddies. The same selection procedure identified 31 cyclonic eddies originating from the Benguela upwelling system (15°S–40°S; 5°E–25°E; Figure 1a) for further analysis.

For each eddy, a timeseries of daily SST, SSS, NCP and wind speed was constructed using the eddy location and radius estimates from the AVISO+ product. For each parameter, the available data were extracted assuming a circular eddy and the median value taken when at least 30% of the data within the eddy were available. An example of the timeseries is given in Figure S1 in Supporting Information S1. To quantify the effect of eddies with respect to the surrounding conditions, daily timeseries of the environmental conditions were also extracted from a circular region three times the radius of the eddy (radii from two to five were tested; Figure S5 in Supporting Information S1), excluding data inside the eddy radius. Median monthly SST, SSS, NCP and wind speeds were calculated from daily timeseries, both for the eddy and the surrounding environment.

2.3. Sea Surface pCO$_2$ Estimates

The sea surface pCO_2 ($pCO_{2(sw)}$) was determined for each month of the eddy trajectories using the South Atlantic Feed Forward Neural Network approach (SA-FNN$_{NCP}$; Ford et al. (2022)). The SA-FNN$_{NCP}$ estimates $pCO_{2(sw)}$ at the base of the mass boundary layer (sub skin $pCO_{2(sw)}$) (Woolf et al., 2016) using non-linear relationships between $pCO_{2(sw)}$ and three environmental drivers; $pCO_{2(atm)}$, SST and NCP, which were constructed for eight static provinces in the South Atlantic Ocean. The SA-FNN$_{NCP}$ was supplied with the monthly median SST and NCP, and the $pCO_{2(atm)}$ for the mean location of the eddy within the month. $pCO_{2(atm)}$ was estimated using the dry mixing ratio of CO_2 from the National Oceanic and Atmospheric Administration Earth System Research Laboratories (NOAA-ESRL) marine boundary layer reference, skin SST and sea level pressure following Dickson et al. (2007). The $pCO_{2(sw)}$ uncertainty was estimated by propagating the $pCO_{2(atm)}$ (1 µatm), satellite SST (0.441°C) and NCP (45 mmol O_2 m^{-2} d^{-1}) (Ford et al., 2021) uncertainties through the SA-FNN$_{NCP}$, and

combined in quadrature with the SA-FNN$_{NCP}$ uncertainty (21.48 µatm) (Ford et al., 2022) using standard uncertainty propagation methods (Taylor, 1997).

2.4. Estimation of the Cumulative Bulk Air-Sea CO$_2$ flux

The air-sea CO$_2$ flux (F) was calculated for each month of the eddy trajectory using a bulk parameterization as:

$$F = k \left(\alpha_W \, p\text{CO}_{2(sw)} - \alpha_s \, p\text{CO}_{2(atm)} \right) \tag{1}$$

where k is the gas transfer velocity estimated from median wind speeds following the parameterization of Nightingale et al. (2000). α_w and α_s are the solubility of CO$_2$ at the base and top of the mass boundary layer at the sea surface (Woolf et al., 2016). α_w was calculated as a function of the skin SST and SSS (Weiss, 1974), applying a cool skin bias of +0.17 K to convert the skin SST to sub skin SST (Donlon et al., 1999; Woolf et al., 2016). α_s was calculated as a function of the eddy skin SST and the SSS with a salinity gradient of +0.1 salinity units between the base and top of the mass boundary layer (Woolf et al., 2016). The CO$_2$ flux calculations were carried out with the open source FluxEngine toolbox (Holding et al., 2019; Shutler et al., 2016) using the "rapid transport" approximation (described in Woolf et al., 2016) at monthly time steps.

The monthly average daily flux of CO$_2$ (mmol C m^{-2} d^{-1}) was multiplied by the number of days and the area of the eddy, assuming a circular eddy with the mean eddy radius, in the respective month. The fluxes (Tg C mon^{-1}) were then added cumulatively to retrieve the net cumulative CO$_2$ flux for each eddy. The uncertainties in $p\text{CO}_{2(sw)}$ (temporally varying), $p\text{CO}_{2(atm)}$ (1 µatm), SST (0.441°C) (Ford et al., 2021) and the gas transfer velocity (assumed to be ±10%; Woolf et al., 2019) were propagated through the cumulative flux calculations using a Monte Carlo uncertainty propagation ($N = 1000$), and the 95% confidence interval (2 standard deviations) extracted as the uncertainty on the cumulative net CO$_2$ flux. These cumulative CO$_2$ flux calculations were repeated for the surrounding environment conditions, assuming the same area as the eddy to estimate the cumulative CO$_2$ flux as if the eddy were not present. A Mann Whitney U-Test was used to assess whether the median percentage differences between the eddy and surrounding environment CO$_2$ flux were significantly different from 0. The Mann Whitney U-Test was selected due to the sample numbers within our study and the lower sensitivity of the test to outliers in the data.

2.5. Thermal and Non-thermal Decomposition of $p\text{CO}_{2(sw)}$ Timeseries

The eddy $p\text{CO}_{2(sw)}$ timeseries was separated into its thermal and non-thermal components as described in Takahashi et al. (2002), where we refer the reader for further details. In brief, the thermal component ($p\text{CO}_{2(therm)}$) was calculated as:

$$p\text{CO}_{2(therm)} = p\text{CO}_{2(sw)} \times e^{\left(0.0423 \times \left(\overline{\text{SST}} - \text{SST} \right) \right)} \tag{2}$$

$\overline{\text{SST}}$ and SST are the mean subskin SST across the eddy timeseries and the monthly subskin SST respectively. The non-thermal component ($p\text{CO}_{2(bio)}$) was calculated as:

$$p\text{CO}_{2(bio)} = \overline{p\text{CO}_{2(sw)}} \times e^{\left(0.0423 \times \left(\text{SST} - \overline{\text{SST}} \right) \right)} \tag{3}$$

$\overline{p\text{CO}_{2(sw)}}$ was the mean $p\text{CO}_{2(sw)}$ for the eddy timeseries. The contributions of the two competing components to the $p\text{CO}_{2(sw)}$ timeseries can be determined from the seasonal amplitude of the $p\text{CO}_{2(therm)}$ and $p\text{CO}_{2(bio)}$;

$$\Delta p\text{CO}_{2(therm)} = \left[p\text{CO}_{2(therm)} \right]_{max} - \left[p\text{CO}_{2(therm)} \right]_{min} \tag{4}$$

$$\Delta p\text{CO}_{2(bio)} = \left[p\text{CO}_{2(bio)} \right]_{max} - \left[p\text{CO}_{2(bio)} \right]_{min} \tag{5}$$

The seasonal amplitudes were calculated using a 12-month moving window for the eddy lifetime, and the ratio between the thermal and non-thermal component (R) was determined as:

$$R = \frac{\Delta p\text{CO}_{2(therm)}}{\Delta p\text{CO}_{2(bio)}} \tag{6}$$

Table 1
The Calculation of the Modification to the South Atlantic Ocean CO₂ Sink That Mesoscale Eddies May Contribute

	Anticyclonic	Cyclonic	
Median cumulative CO_2 flux (Figures 1b and 1d; Tg C per eddy)	−0.54 (IQR = 0.38)	−0.27 (IQR = 0.17)	
Median percentage change in CO_2 flux compared to surrounding environment (Figure 2c; %)	−3.7 (IQR = 5.2)	−1.4 (IQR = 4.8)	
Additional flux into eddy (Tg C per eddy)	−0.020 ± 0.015	−0.004 ± 0.006	
Mean eddy lifetime (yr)	2.5	1.7	
Additional flux into eddy per year (Tg C yr^{-1})	−0.008 ± 0.006	−0.002 ± 0.003	
Spawn Rate (yr)	6 (Lutjeharms, 2006)	4 (Chaigneau et al., 2009)	
Additional flux into eddies (Tg C yr^{-1})	−0.05 ± 0.03	−0.01 ± 0.02	
			Total
South Atlantic Ocean CO_2 sink estimate of Ford et al. (2022) (−76 ± 8 Tg C yr^{-1}) 20°S–44°S	−0.06 ± 0.04%	−0.02 ± 0.02%	−0.08 ± 0.04%
South Atlantic Ocean CO_2 sink estimate of Woolf et al. (2019) and Holding et al. (2019) (−261 ± 28 Tg C yr^{-1}) 20°S–44°S	−0.020 ± 0.015%	−0.005 ± 0.008%	−0.030 ± 0.013%

Note. The median percentage change in the eddy flux compared to the surrounding environment is converted to a median Tg C yr^{-1} equivalent and compared to two estimates of the South Atlantic CO_2 sink in the region the eddies propagate. IQR is the interquartile range.

In cases where R is greater (less) than 1, the thermal (non-thermal) contribution was the dominant driver. The anomaly in R was determined by subtracting the mean R across the eddy's lifetime.

3. Results

The accurate estimation of $pCO_{2(sw)}$ by the SA-FNN$_{NCP}$ is an important component of the air-sea CO_2 flux calculation. A comparison between the SA-FNN$_{NCP}$ estimated and in situ $pCO_{2(sw)}$ within both anticyclonic ($n = 6$) and cyclonic eddies ($n = 2$; Figure S2 in Supporting Information S1) was therefore performed. The showed that the SA-FNN$_{NCP}$ was accurate and precise within anticyclonic eddies (root mean square deviation = 10 μatm; bias = 0 μatm) but larger differences were apparent in $pCO_{2(sw)}$ for the cyclonic eddies, albeit from just two crossovers (root mean square deviation = 21 μatm; bias 11 μatm). The comparison provides confidence in the resulting air-sea CO_2 flux estimates.

The analysis of the eddy cumulative CO_2 flux showed both anticyclonic (Agulhas; Table 1) and cyclonic (Benguela; Table 1) eddies acted as net CO_2 sinks over their lifetime (Figures 1b and 1d). Anticyclonic eddies displayed an exponential decay in the increase of the net cumulative CO_2 sink, compared to a more linear increase in cyclonic eddies using the same functional equation (Figures 1c and 1e).

The anomaly in the thermal to non-thermal contribution to $pCO_{2(sw)}$ variability in anticyclonic eddies changed over their lifetimes (Figure 2a), where a positive anomaly indicates an increasing dominance of temperature on controlling $pCO_{2(sw)}$. For cyclonic eddies the anomaly in the thermal to non-thermal component ratio, did not change significantly over time (Figure 2b).

The anticyclonic (−3.7%, Mann-Whitney U-Test, $p < 0.001$, $n = 36$) and cyclonic (−1.4%, Mann-Whitney U-Test, $p = 0.007$, $n = 31$) eddies significantly enhanced the cumulative CO_2 sink compared to the water surrounding each eddy (Figure 2c). No significant differences in this enhancement were observed between anticyclonic and cyclonic eddies (Figure 2c; Mann-Whitney U-Test, $p = 0.16$), although the median anticyclonic modification was double that of the cyclonic eddies (Figure 2c).

4. Discussion

To our knowledge, this is the first study to provide an observation-based assessment of the cumulative net CO_2 flux of a large number (67) of long-lived mesoscale eddies. The trajectory of 36 anticyclonic eddies was followed over their lifetime and showed that they were a net cumulative CO_2 sink (median = 0.54 Tg C per eddy; Table 1). This result is consistent with the lower end of values from the literature for anticyclonic (Agulhas) eddies which
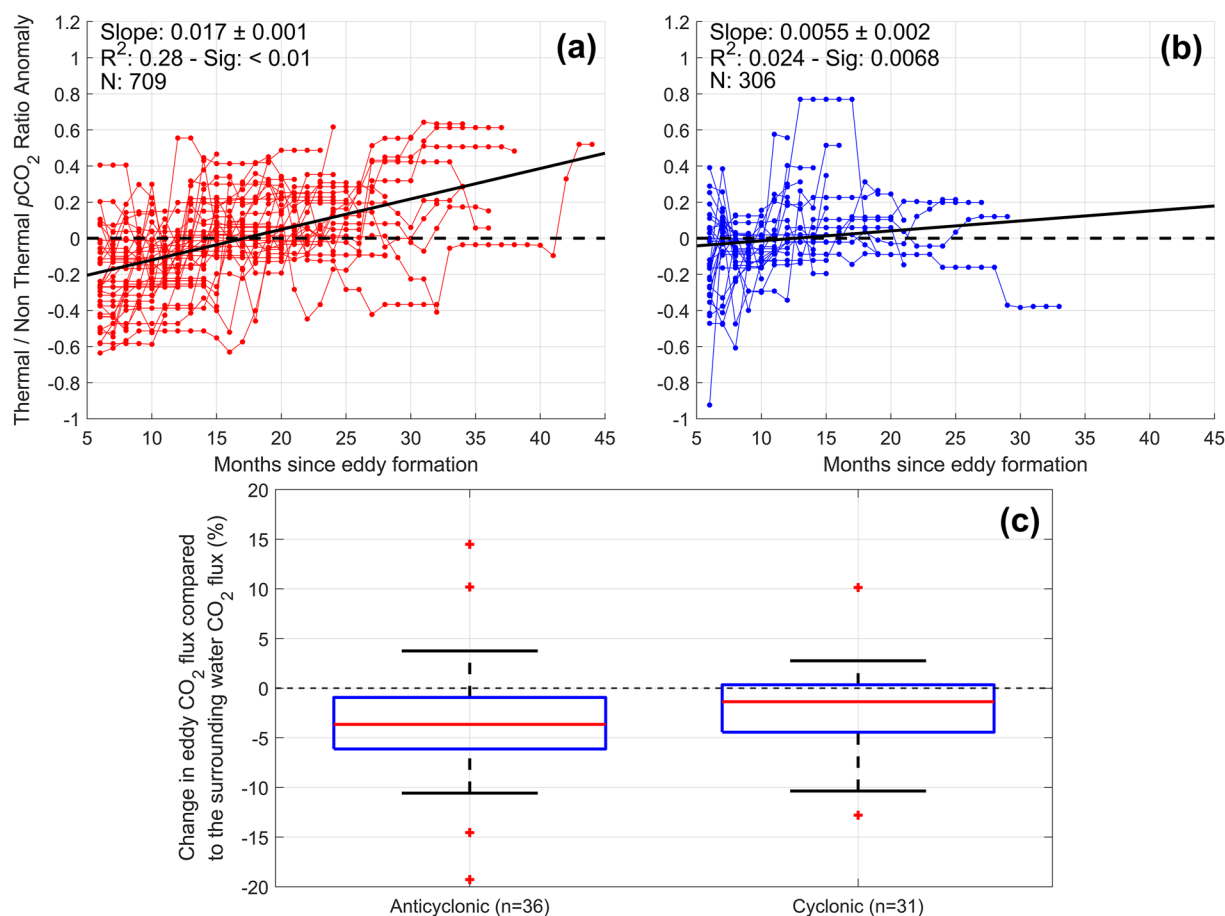
Figure 2. (a) Anomaly in the 12-month running thermal to the non-thermal ratio of $pCO_{2(sw)}$ for the 36 anticyclonic eddies. Black solid line indicates the linear fit since the formation of the eddy. Black dashed line indicates an anomaly of 0. Statistics within the plot are: Slope is the slope of the linear fit, R^2 is the coefficient of determination, Sig is the significance of the linear fit and N is number of samples. (b) Same as (a) but for the 31 cyclonic eddies. (c) Box plots indicating the percent change in the cumulative net CO_2 flux at eddy dissipation with respect to the waters surrounding the eddy. Red line indicates the median, blue box indicates the 25th and 75th percentile and whiskers show the minimum and maximum non-outlier values. Red crosses indicate outliers that are more than 1.5 times the interquartile range from the 25th and 75th percentiles. Negative percentages indicate a stronger flux, where positive percentages indicate a weaker flux.

have identified them as a net sink for CO_2 varying from ~0.6 to ~1.4 Tg C (median = 1.26 Tg C per eddy; Figure 1b; Orselli, Kerr, et al., 2019). The results of the Orselli, Kerr, et al. (2019) study were based on extrapolation of a snapshot of the eddies CO_2 uptake potential from ship observations that crossed the paths of six eddies. Two of these eddies were tracked in our study (V1, V3; Figure 1b) and identified as CO_2 sinks of 0.64 and 0.40 Tg C compared to 1.34 and 1.36 Tg C by Orselli, Kerr, et al. (2019). The eddies sampled by Orselli, Kerr, et al. (2019) were in austral winter when they were a strong CO_2 sink. In our study, the seasonal variability in the CO_2 flux is captured, where eddies were stronger sinks in winter and weaker sinks for CO_2 in summer, which likely explains the lower cumulative CO_2 flux. This seasonality in the CO_2 flux would partially be due to seasonal SST and wind speed cycles, where cooler SST increases CO_2 solubility (e.g., Figures S1a and S1b in Supporting Information S1) and elevated wind speeds increase gas transfer during winter (Kitidis et al., 2019).

Both the anticyclonic and cyclonic eddies showed an increasing cumulative CO_2 sink over their lifetime (Figures 1c and 1e). For the former, the rate of CO_2 uptake decreased exponentially over this period (Figure 1c). This result is consistent with the geographical propagation of the eddies in the oligotrophic South Atlantic gyre (Figure 1a), and eddy stirring of the environment (McGillicuddy, 2016). The significant increase in the anomalies of the seasonal thermal to non-thermal $pCO_{2(sw)}$ ratio (becoming more influenced by temperature; Figure 2a) was found to be mainly driven by a relative reduction in the non-thermal contribution (not shown) and highlights the changing role of biological activity and/or circulation over time as the eddies propagated into the gyre. Carvalho et al. (2019) showed that the phytoplankton community structure changed as the eddies aged, where younger

anticyclonic (Agulhas) eddies were dominated by haptophytes (small flagellates) followed by prokaryotes. The shift in community structure was attributed to a decrease in nutrient availability at the surface, whereby prokaryotes are better adapted to lower nutrient concentrations. Sarkar et al. (2021) highlighted that haptophytes are crucial for the biological CO_2 drawdown in the Agulhas retroflection, reinforcing a weaker biological pump as the eddies evolve. In contrast, the cyclonic eddies displayed a linear increase in the cumulative CO_2 sink (Figure 1e). This signature may be because the cyclonic eddies do not propagate as far as anticyclonic eddies into the South Atlantic gyre (Figure 1a), which is also illustrated by no significant change in the thermal to non-thermal $pCO_{2(sw)}$ ratio anomaly (Figure 2b).

Both the anticyclonic and cyclonic eddies were shown to significantly increase the CO_2 drawdown in the South Atlantic Ocean (Figure 2c), compared to the surrounding environment. Jones et al. (2017) showed that both anticyclonic and cyclonic eddies were hotspots for CO_2 drawdown in the Antarctic Circumpolar Current. Dufois et al. (2016) examined chl a variability in anticyclonic eddies and showed that the first two modes of spatial variability were consistent with eddy stirring, and the third mode highlighted the mesoscale modification. In our study, by comparing the cumulative CO_2 fluxes of the eddies to a theoretical eddy consisting of surface waters surrounding the eddy, the mesoscale modulation of the air-sea CO_2 flux was quantified. We showed this modulation to increase the CO_2 sink into anticyclonic and cyclonic eddies by 3.7% and 1.4% respectively (Figure 2c).

The cyclonic eddies generally showed lower SST, and higher NCP (Figures S3 and S4 in Supporting Information S1) compared to the surrounding waters, suggesting that both biological and physical processes amplify the CO_2 sink. Chen et al. (2007) showed in the North Pacific that $pCO_{2(sw)}$ was elevated at the core of a cyclonic eddy, due to the upwelling of CO_2 rich waters into the surface layer and the eddy acting as a weaker CO_2 sink compared to the surrounding waters. By comparison, Lovecchio et al. (2022) identified that cyclonic eddies around the Canary upwelling system entrain nearshore nutrient rich waters into the eddy core at formation. Mesoscale upwelling of nutrients was a small component of the total nutrients sustaining the biological production. This suggests that the biological CO_2 drawdown throughout the eddy lifetime is largely supported by the initial nutrient input which ultimately enhances the CO_2 sink through both the physical and biological signatures.

The anticyclonic eddies were associated with elevated SST at formation, which rapidly changed to depressed SST for the remainder of their lifetimes (Figure S3 in Supporting Information S1) compared to the surrounding waters. NCP remained lower than the surroundings (Figure S4 in Supporting Information S1). These characteristics suggest opposing physical and biological forces that modify the air-sea CO_2 flux. Similarly, Laxenaire et al. (2019) showed that the SST anomaly associated with surface water of an anticyclonic (Agulhas) eddy switched from positive to negative over its lifetime, also implying a change from a CO_2 source to sink as it propagated over the South Atlantic basin. This indicates that the physical component exerts the greatest control on amplifying the air-sea CO_2 sink into these anticyclonic eddies. The magnitude of SST differences in anticyclonic eddies compared to the surrounding environment were generally double that of cyclonic eddies which is indicative of the mechanism by which anticyclonic eddies enhance the CO_2 sink more than cyclonic eddies.

This study has identified the capacity for eddies to modify the air-sea CO_2 flux (Figure 2c) which is driven by intrinsic differences between individual eddies (Figures S3 and S4 in Supporting Information S1). Lehahn et al. (2011) observed an isolated patch of elevated chl a associated with an anticyclonic eddy that was transported into the South Atlantic gyre, suggesting enhanced biological drawdown of CO_2, though it was not possible to identify if this is a common feature of all anticyclonic eddies. Entrainment of nutrient rich nearshore waters into the cyclonic eddies (Lovecchio et al., 2022) is likely to be highly variable depending on the location and interaction with other water bodies and the time of year, which will in turn lead to a different biological response and therefore air-sea CO_2 flux. Many mesoscale eddy studies are limited by the availability of in situ data (Jones et al., 2017; Laxenaire et al., 2019; Orselli, Kerr, et al., 2019). The expanding use of Biogeochemical-Argo profilers, especially those with pH sensors (Roemmich et al., 2019), is improving the potential to assess the air-sea CO_2 flux both globally and regionally (Gray et al., 2018). A synergy of in situ and satellite observations is the most comprehensive means of studying the processes by which mesoscale eddies modify the air-sea CO_2 flux.

Based on a recent assessment of the South Atlantic Ocean (20°S–44°S) by Ford et al. (2022), which estimated the region to be a CO_2 sink of 76 Tg C yr^{-1}, the long-lived anticyclonic (Agulhas) eddies assuming six eddies are released per year (Lutjeharms, 2006) would contribute 1.3 Tg C yr^{-1} (1.7%; Table 1). Orselli, Kerr, et al. (2019) identified that six anticyclonic (Agulhas) eddies contributed 2.5 Tg C yr^{-1} (3.3%) to the CO_2 sink. Our contribution is lower because seasonal variability in the CO_2 flux was captured.

We found that anticyclonic and cyclonic eddies enhance the oceanic CO_2 sink into the South Atlantic Ocean (20°S–44°S) by 0.08 ± 0.04% (Table 1). Globally, long lived mesoscale eddies, make up 0.4% of the eddy trajectories in the AVISO+ data set (Pegliasco et al., 2022). This suggests that the effect of all eddies on the CO_2 flux and net oceanic sink is likely to be globally significant. Eddy kinetic energy, as a proxy for mesoscale eddy occurrence, has been increasing at a rate between 2% and 5% per decade (Martínez-Moreno et al., 2021), indicating that the role of mesoscale eddies on the oceanic CO_2 sink may be becoming more significant. In the context of climate change and increasing global temperatures, further work is required to quantify the influence of these changes on the ocean CO_2 sink.

5. Conclusions

Our analysis presents a novel approach to assess the impact of long-lived mesoscale eddies on the air-sea CO_2 flux in the South Atlantic Ocean. Using satellite observations, in situ data and Lagrangian tracking we show that anticyclonic and cyclonic eddies are cumulative net CO_2 sinks of 0.54 and 0.27 Tg C per eddy (median values), respectively. Anticyclonic eddies exhibited an exponential decay in the rate of CO_2 uptake, and significant changes in the thermal to non-thermal drivers of the $pCO_{2(sw)}$ ratio anomaly. This shows that the thermal and biological contributions to the CO_2 sink variability change as the eddies age and propagate over different geographic trajectories in the South Atlantic gyre. The cyclonic eddies showed a more linear rate of CO_2 uptake, and there was no significant change in the drivers of the seasonal $pCO_{2(sw)}$ ratio anomaly.

Both anticyclonic and cyclonic eddies amplified the CO_2 sink compared to the surrounding environment by 3.7% and 1.4%, respectively. For the anticyclonic eddies, physical drivers increased the CO_2 sink, whereas the biological component reduced the uptake. In cyclonic eddies both physical and biological components worked synergistically to increase the CO_2 sink. Accounting for their typical frequencies, long-lived mesoscale eddies significantly amplify the CO_2 sink into the South Atlantic Ocean (20°S–44°S) by 0.08 ± 0.04%. Although this modification appears small, long-lived eddies make up 0.4% of eddies in the global oceans, and therefore the amplification of the global CO_2 sink from all eddies is likely to be much larger than previously estimated. The inclusion of these mesoscale features would improve estimates of the role of the global ocean in the uptake of anthropogenic CO_2.

Data Availability Statement

Daily Moderate Resolution Imaging Spectroradiometer on Aqua (MODIS-A) estimates of chlorophyll-a (NASA OBPG, 2017a), photosynthetically active radiation (NASA OBPG, 2017b) and sea surface temperature (NASA OBPG, 2015) are available from the National Aeronautics Space Administration (NASA) ocean color website (https://oceancolor.gsfc.nasa.gov/). Modeled sea surface salinity from the Copernicus Marine Environment Modelling Service (CMEMS) global ocean physics reanalysis product (GLORYS12V1) are available from CMEMS (CMEMS, 2021). The CCMP daily wind speed products are available from Remote Sensing Systems (www.remss.com/measurements/ccmp; Wentz et al., 2015). In situ GO-SHIP DIC and TA samples can be downloaded from the NOAA/NODC data centre (https://www.ncei.noaa.gov/access/ocean-carbon-data-system/oceans/RepeatSections/). FORSA in situ $pCO_{2(sw)}$ data can be retrieved from PANGAEA (Orselli et al., 2023). Optimum Interpolated SST (OISST) v2 (Reynolds et al., 2002) data used in the reanalysis of $pCO_{2(sw)}$ can be downloaded from https://psl.noaa.gov/data/gridded/data.noaa.oisst.v2.html. The AVISO+ Mesoscale Eddy Product META3.1exp can be downloaded from https://doi.org/10.24400/527896/a01-2021.001 (Pegliasco et al., 2021).

References

Angel-Benavidez, I. M., Pilo, G. S., Dias, F. B., & Garcia, C. A. E. (2016). Influência de vórtices na concentração de clorofila da confluência Brasil-Malvinas: Mecanismos inferidos por sensoriamento remoto. *Brazilian Journal of Aquatic Science and Technology*, *20*(1). https://doi.org/10.14210/bjast.v20n1.4782

Arhan, M., Speich, S., Messager, C., Dencausse, G., Fine, R., & Boye, M. (2011). Anticyclonic and cyclonic eddies of subtropical origin in the subantarctic zone south of Africa. *Journal of Geophysical Research*, *116*(11), 1–22. https://doi.org/10.1029/2011JC007140

Carvalho, A. da C. de O., Mendes, C. R. B., Kerr, R., de Azevedo, J. L. L., Galdino, F., & Tavano, V. M. (2019). The impact of mesoscale eddies on the phytoplankton community in the South Atlantic Ocean: HPLC-CHEMTAX approach. *Marine Environmental Research*, *144*, 154–165. https://doi.org/10.1016/j.marenvres.2018.12.003

Chaigneau, A., Eldin, G., & Dewitte, B. (2009). Eddy activity in the four major upwelling systems from satellite altimetry (1992–2007). *Progress in Oceanography*, *83*(1–4), 117–123. https://doi.org/10.1016/j.pocean.2009.07.012

Chelton, D. B., Schlax, M. G., & Samelson, R. M. (2011). Global observations of nonlinear mesoscale eddies. *Progress in Oceanography*, *91*(2), 167–216. https://doi.org/10.1016/j.pocean.2011.01.002

Chen, F., Cai, W. J., Benitez-Nelson, C., & Wang, Y. (2007). Sea surface pCO$_2$-SST relationships across a cold-core cyclonic eddy: Implications for understanding regional variability and air-sea gas exchange. *Geophysical Research Letters*, *34*(10), L10603. https://doi.org/10.1029/2006GL028058

CMEMS. (2021). Copernicus Marine Modelling Service global ocean physics reanalysis product (GLORYS12V1) [Dataset]. Copernicus Marine Modelling Service. https://doi.org/10.48670/moi-00021

Dickson, A. G., Sabine, C. L., & Christian, J. R. (2007). *Guide to best practices for ocean CO$_2$ measurements*. IOCCP report no. 8 (Vol. 3, p. 191). PICES Special Publication.

Donlon, C. J., Nightingale, T. J., Sheasby, T., Turner, J., Robinson, I. S., & Emergy, W. J. (1999). Implications of the oceanic thermal skin temperature deviation at high wind speed. *Geophysical Research Letters*, *26*(16), 2505–2508. https://doi.org/10.1029/1999GL900547

Dufois, F., Hardman-Mountford, N. J., Greenwood, J., Richardson, A. J., Feng, M., & Matear, R. J. (2016). Anticyclonic eddies are more productive than cyclonic eddies in subtropical gyres because of winter mixing. *Science Advances*, *2*(5), 1–7. https://doi.org/10.1126/sciadv.1600282

Ford, D. J., Tilstone, G. H., Shutler, J. D., & Kitidis, V. (2022). Derivation of seawater pCO$_2$ from net community production identifies the South Atlantic Ocean as a CO$_2$ source. *Biogeosciences*, *19*(1), 93–115. https://doi.org/10.5194/bg-19-93-2022

Ford, D. J., Tilstone, G. H., Shutler, J. D., Kitidis, V., Lobanova, P., Schwarz, J., et al. (2021). Wind speed and mesoscale features drive net autotrophy in the South Atlantic Ocean. *Remote Sensing of Environment*, *260*, 112435. https://doi.org/10.1016/j.rse.2021.112435

Frenger, I., Gruber, N., Knutti, R., & Münnich, M. (2013). Imprint of Southern Ocean eddies on winds, clouds and rainfall. *Nature Geoscience*, *6*(8), 608–612. https://doi.org/10.1038/ngeo1863

Gaube, P., McGillicuddy, D. J., Chelton, D. B., Behrenfeld, M. J., & Strutton, P. G. (2014). Regional variations in the influence of mesoscale eddies on near-surface chlorophyll. *Journal of Geophysical Research: Oceans*, *119*(12), 8195–8220. https://doi.org/10.1002/2014JC010111

Gray, A. R., Johnson, K. S., Bushinsky, S. M., Riser, S. C., Russell, J. L., Talley, L. D., et al. (2018). Autonomous biogeochemical floats detect significant carbon dioxide outgassing in the high-latitude Southern Ocean. *Geophysical Research Letters*, *45*(17), 9049–9057. https://doi.org/10.1029/2018GL078013

Guerra, L. A. A., Paiva, A. M., & Chassignet, E. P. (2018). On the translation of Agulhas rings to the western South Atlantic Ocean. *Deep-Sea Research Part I: Oceanographic Research Papers*, *139*, 104–113. https://doi.org/10.1016/j.dsr.2018.08.005

Holding, T., Ashton, I. G., Shutler, J. D., Land, P. E., Nightingale, P. D., Rees, A. P., et al. (2019). The FluxEngine air–sea gas flux toolbox: Simplified interface and extensions for in situ analyses and multiple sparingly soluble gases. *Ocean Science*, *15*(6), 1707–1728. https://doi.org/10.5194/os-15-1707-2019

Jones, E. M., Hoppema, M., Strass, V., Hauck, J., Salt, L., Ossebaar, S., et al. (2017). Mesoscale features create hotspots of carbon uptake in the Antarctic Circumpolar Current. *Deep-Sea Research Part II: Topical Studies in Oceanography*, *138*, 39–51. https://doi.org/10.1016/j.dsr2.2015.10.006

Kitidis, V., Shutler, J. D., Ashton, I., Warren, M., Brown, I., Findlay, H., et al. (2019). Winter weather controls net influx of atmospheric CO$_2$ on the north-west European shelf. *Scientific Reports*, *9*(1), 20153. https://doi.org/10.1038/s41598-019-56363-5

Landschützer, P., Gruber, N., Bakker, D. C. E., & Schuster, U. (2014). Recent variability of the global ocean carbon sink. *Global Biogeochemical Cycles*, *28*(9), 927–949. https://doi.org/10.1002/2014GB004853

Laxenaire, R., Speich, S., & Stegner, A. (2019). Evolution of the thermohaline structure of one Agulhas ring reconstructed from satellite altimetry and Argo floats. *Journal of Geophysical Research: Oceans*, *124*(12), 8969–9003. https://doi.org/10.1029/2018JC014426

Lehahn, Y., D'Ovidio, F., Lévy, M., Amitai, Y., & Heifetz, E. (2011). Long range transport of a quasi isolated chlorophyll patch by an Agulhas ring. *Geophysical Research Letters*, *38*(16). https://doi.org/10.1029/2011GL048588

Liu, F., Yin, K., He, L., Tang, S., & Yao, J. (2018). Influence on phytoplankton of different developmental stages of mesoscale eddies off eastern Australia. *Journal of Sea Research*, *137*, 1–8. https://doi.org/10.1016/j.seares.2018.03.004

Lovecchio, E., Gruber, N., Münnich, M., & Frenger, I. (2022). On the processes sustaining biological production in the offshore propagating eddies of the northern canary upwelling system. *Journal of Geophysical Research: Oceans*, *127*(2), 1–28. https://doi.org/10.1029/2021JC017691

Lutjeharms, J. R. E. (2006). *The Agulhas current*. Springer Berlin. https://doi.org/10.1007/3-540-37212-1

Martínez-Moreno, J., Hogg, A. M. C., England, M. H., Constantinou, N. C., Kiss, A. E., & Morrison, A. K. (2021). Global changes in oceanic mesoscale currents over the satellite altimetry record. *Nature Climate Change*, *11*(5), 397–403. https://doi.org/10.1038/s41558-021-01006-9

Mason, E., Pascual, A., & McWilliams, J. C. (2014). A new sea surface height—Based code for oceanic mesoscale eddy tracking. *Journal of Atmospheric and Oceanic Technology*, *31*(5), 1181–1188. https://doi.org/10.1175/JTECH-D-14-00019.1

McGillicuddy, D. J. (2016). Mechanisms of physical-biological-biogeochemical interaction at the oceanic mesoscale. *Annual Review of Marine Science*, *8*(1), 125–159. https://doi.org/10.1146/annurev-marine-010814-015606

Morel, A. (1991). Light and marine photosynthesis: A spectral model with geochemical and climatological implications. *Progress in Oceanography*, *26*(3), 263–306. https://doi.org/10.1016/0079-6611(91)90004-6

NASA OBPG. (2015). MODIS-Aqua level 3 SST thermal IR daily 4 km daytime v2014.0 [Dataset]. NASA Physical Oceanography DAAC. https://doi.org/10.5067/MODSA-1D4D4

NASA OBPG. (2017a). MODIS-Aqua level 3 mapped chlorophyll data version R2018.0 [Dataset]. NASA Ocean Biology DAAC. https://doi.org/10.5067/AQUA/MODIS/L3M/CHL/2018

NASA OBPG. (2017b). MODIS-Aqua level 3 mapped photosynthetically available radiation data version R2018.0 [Dataset]. NASA Ocean Biology DAAC. https://doi.org/10.5067/AQUA/MODIS/L3M/PAR/2018

Nencioli, F., Dall'Olmo, G., & Quartly, G. D. (2018). Agulhas ring transport efficiency from combined satellite altimetry and Argo profiles. *Journal of Geophysical Research: Oceans*, *123*(8), 5874–5888. https://doi.org/10.1029/2018JC013909

Nightingale, P. D., Malin, G., Law, C. S., Watson, A. J., Liss, P. S., Liddicoat, M. I., et al. (2000). In situ evaluation of air-sea gas exchange parameterizations using novel conservative and volatile tracers. *Global Biogeochemical Cycles*, *14*(1), 373–387. https://doi.org/10.1029/1999GB900091

Orselli, I. B. M., Goyet, C., Kerr, R., de Azevedo, J. L. L., Araujo, M., Galdino, F., et al. (2019). The effect of Agulhas eddies on absorption and transport of anthropogenic carbon in the South Atlantic Ocean. *Climate*, *7*(6), 1–25. https://doi.org/10.3390/CLI7060084

Orselli, I. B. M., Kerr, R., de Azevedo, J. L. L., Galdino, F., Araujo, M., & Garcia, C. A. E. (2019). The sea-air CO$_2$ net fluxes in the South Atlantic Ocean and the role played by Agulhas eddies. *Progress in Oceanography*, *170*, 40–52. https://doi.org/10.1016/j.pocean.2018.10.006

Orselli, I. B. M., Kerr, R., de Azevedo, J. L. L., Galdino, F., Araujo, M., & Garcia, C. A. E. (2023). Continuous pCO2 and seasea-air CO2 net fluxes from the Following Ocean Rings in the South Atlantic (FORSA) cruise [Dataset]. PANGAEA. https://doi.org/10.1594/PANGAEA.957502

Pegliasco, C., Delepoulle, A., & Faugere, Y. (2021). Mesoscale eddy trajectories atlas delayed-time all satellites: Version META3.1exp DT allsat [Dataset]. AVISO+. https://doi.org/10.24400/527896/a01-2021.001

Pegliasco, C., Delepoulle, A., Mason, E., Morrow, R., Faugère, Y., & Dibarboure, G. (2022). META3.1exp: A new global mesoscale eddy trajectory atlas derived from altimetry. *Earth System Science Data*, *14*(3), 1087–1107. https://doi.org/10.5194/essd-14-1087-2022

Pezzi, L. P., de Souza, R. B., Santini, M. F., Miller, A. J., Carvalho, J. T., Parise, C. K., et al. (2021). Oceanic eddy-induced modifications to air–sea heat and CO_2 fluxes in the Brazil-Malvinas Confluence. *Scientific Reports*, *11*(1), 10648. https://doi.org/10.1038/s41598-021-89985-9

Reynolds, R. W., Rayner, N. A., Smith, T. M., Stokes, D. C., & Wang, W. (2002). An improved in situ and satellite SST analysis for climate. *Journal of Climate*, *15*(13), 1609–1625. https://doi.org/10.1175/1520-0442(2002)015<1609:AIISAS>2.0.CO;2

Roemmich, D., Alford, M. H., Claustre, H., Johnson, K. S., King, B., Moum, J., et al. (2019). On the future of Argo: A global, full-depth, multi-disciplinary array. *Frontiers in Marine Science*, *6*, 1–28. https://doi.org/10.3389/fmars.2019.00439

Roughan, M., Keating, S. R., Schaeffer, A., Cetina Heredia, P., Rocha, C., Griffin, D., et al. (2017). A tale of two eddies: The biophysical characteristics of two contrasting cyclonic eddies in the East Australian Current System. *Journal of Geophysical Research: Oceans*, *122*(3), 2494–2518. https://doi.org/10.1002/2016JC012241

Rubio, A., Blanke, B., Speich, S., Grima, N., & Roy, C. (2009). Mesoscale eddy activity in the southern Benguela upwelling system from satellite altimetry and model data. *Progress in Oceanography*, *83*(1–4), 288–295. https://doi.org/10.1016/j.pocean.2009.07.029

Sarkar, A., Mishra, R., Bhaskar, P. V., Anilkumar, N., Sabu, P., & Soares, M. (2021). Potential role of major phytoplankton communities on pCO2 modulation in the Indian sector of Southern Ocean. *Thalassas*, *37*(2), 531–548. https://doi.org/10.1007/s41208-021-00323-2

Shutler, J. D., Land, P. E., Piolle, J. F., Woolf, D. K., Goddijn-Murphy, L., Paul, F., et al. (2016). FluxEngine: A flexible processing system for calculating atmosphere-ocean carbon dioxide gas fluxes and climatologies. *Journal of Atmospheric and Oceanic Technology*, *33*(4), 741–756. https://doi.org/10.1175/JTECH-D-14-00204.1

Smyth, T. J., Tilstone, G. H., & Groom, S. B. (2005). Integration of radiative transfer into satellite models of ocean primary production. *Journal of Geophysical Research C: Oceans*, *110*(10), 1–11. https://doi.org/10.1029/2004JC002784

Song, H., Marshall, J., Munro, D. R., Dutkiewicz, S., Sweeney, C., McGillicuddy, D. J., & Hausmann, U. (2016). Mesoscale modulation of air-sea CO_2 flux in Drake Passage. *Journal of Geophysical Research: Oceans*, *121*(9), 6635–6649. https://doi.org/10.1002/2016JC011714

Souza, R., Pezzi, L., Swart, S., Oliveira, F., & Santini, M. (2021). Air-sea interactions over eddies in the Brazil-Malvinas confluence. *Remote Sensing*, *13*(7), 1335. https://doi.org/10.3390/rs13071335

Takahashi, T., Sutherland, S. C., Sweeney, C., Poisson, A., Metzl, N., Tilbrook, B., et al. (2002). Global sea–air CO_2 flux based on climatological surface ocean pCO2, and seasonal biological and temperature effects. *Deep Sea Research Part II: Topical Studies in Oceanography*, *49*(9–10), 1601–1622. https://doi.org/10.1016/S0967-0645(02)00003-6

Taylor, J. R. (1997). *An introduction to error analysis*. University Science Books.

Tilstone, G. H., Xie, Y. Y., Robinson, C., Serret, P., Raitsos, D. E., Powell, T., et al. (2015). Satellite estimates of net community production indicate predominance of net autotrophy in the Atlantic Ocean. *Remote Sensing of Environment*, *164*, 254–269. https://doi.org/10.1016/j.rse.2015.03.017

Weiss, R. F. (1974). Carbon dioxide in water and seawater: The solubility of a non-ideal gas. *Marine Chemistry*, *2*(3), 203–215. https://doi.org/10.1016/0304-4203(74)90015-2

Wentz, F. J., Scott, J., Hoffman, R., Leidner, M., Atlas, R., & Ardizzone, J. (2015). Remote Sensing Systems Cross-Calibrated Multi-Platform (CCMP) 6-hourly ocean vector wind analysis product on 0.25 deg grid, Version 2.0 [Dataset]. Remote Sensing Systems. Retrieved from www.remss.com/measurements/ccmp

Woolf, D. K., Land, P. E., Shutler, J. D., Goddijn-Murphy, L. M., & Donlon, C. J. (2016). On the calculation of air-sea fluxes of CO_2 in the presence of temperature and salinity gradients. *Journal of Geophysical Research: Oceans*, *121*(2), 1229–1248. https://doi.org/10.1002/2015JC011427

Woolf, D. K., Shutler, J. D., Goddijn-Murphy, L., Watson, A. J., Chapron, B., Nightingale, P. D., et al. (2019). Key uncertainties in the recent air-sea flux of CO_2. *Global Biogeochemical Cycles*, *33*(12), 1548–1563. https://doi.org/10.1029/2018GB006041

References From the Supporting Information

Dickson, A. G. (1990). Standard potential of the Standard potential of the reaction—AgCl(s) + 1/2H₂(g) = Ag(s) + HCl(aq) and the standard acidity constant of the ion HSO₄⁻ in synthetic sea-water from 273.15-K to 318.15-K. *The Journal of Chemical Thermodynamics*, *22*(2), 113–127. https://doi.org/10.1016/0021-9614(90)90074-Z

Goddijn-Murphy, L. M., Woolf, D. K., Land, P. E., Shutler, J. D., & Donlon, C. (2015). The OceanFlux Greenhouse Gases methodology for deriving a sea surface climatology of CO_2 fugacity in support of air-sea gas flux studies. *Ocean Science*, *11*(4), 519–541. https://doi.org/10.5194/os-11-519-2015

van Heuven, S., Pierrot, D., Rae, J. W. B., Lewis, E., & Wallace, D. W. R. (2011). *MATLAB Program developed for CO_2 system calculations* [Software]. Oak Ridge National Laboratory, Carbon Dioxide Information Analysis Center. https://doi.org/10.3334/CDIAC/otg.CO2SYS_MATLAB_v1.1

Lewis, E., Wallace, D., & Allison, L. J. (1998). Program developed for CO_2 system calculations. https://doi.org/10.2172/639712

Orr, J. C., Epitalon, J.-M., Dickson, A. G., & Gattuso, J.-P. (2018). Routine uncertainty propagation for the marine carbon dioxide system. *Marine Chemistry*, *207*, 84–107. https://doi.org/10.1016/j.marchem.2018.10.006

Sharp, J. D., Pierrot, D., Humphreys, M. P., Epitalon, J.-M., Orr, J. C., Lewis, E. R., & Wallace, D. W. R. (2021). CO2SYSv3 for MATLAB [Software]. https://doi.org/10.5281/ZENODO.4774718

Waters, J., Millero, F. J., & Woosley, R. J. (2014). Corrigendum to "The free proton concentration scale for seawater pH", [MARCHE: 149 (2013) 8–22]. *Marine Chemistry*, *165*, 66–67. https://doi.org/10.1016/j.marchem.2014.07.004